Research Article Vol. 28, No. 1 / 6 January 2020 / Optics Express 626
Optics EXPRESS

New testing and calculation method for determination viscoelasticity of optical glass

YINGYING ZHANG,[1,2] SHAOHUI YIN,[1,*] RONGGUANG LIANG,[2] HONG LUO,[1] HUAPAN XIAO,[2] AND NINGXIAO YUAN[3]

[1]College of Mechanical & Vehicle Engineering, Hunan University, Changsha, China
[2]College of Optical Sciences, University of Arizona, Tucson, Arizona 85719, USA
[3]Mettler-Toledo Company, Guangzhou, China
[*]yinshaohui@hnu.edu.cn

Abstract: Viscoelastic properties of glass within molding temperatures, such as shear relaxation modulus and bulk relaxation modulus, are key factors to build successful numerical model, predict forming process, and determine optimal process parameters for precision glass molding. However, traditional uniaxial compression creep tests with large strains are very limited in obtaining high-accuracy viscoelastic data of glass, due to the declining compressive stress caused by the increasing cross-sectional area of specimen in testing process. Besides, existing calculation method has limitation in transforming creep data to viscoelasticity data, especially when Poisson's ratio is unknown at molding temperature, which further induces a block to characterize viscoelastic parameter. This study proposes a systematic acquisition method for high-precision viscoelastic data, including creep testing, viscoelasticity calculation, and finite element verification. A minimal uniaxial creep testing (MUCT) method based on thermo-mechanical analysis (TMA) instrument is first built to obtain ideal and accurate creep data, by keeping compressive stress as a constant. A new calculation method on viscoelasticity determination is then proposed to derive shear relaxation modulus without the need of knowing bulk modulus or Poisson's ratio, which, compared with traditional method, extends the application range of viscoelasticity calculation. After determination, the obtained viscoelastic data are further incorporated into a numerical simulation model of MUCT to verify the accuracy of the determined viscoelasticity. Base on the great consistence between simulated and measured results (uniaxial creep displacement), the proposed systematic acquisition method can be used as a high accuracy viscoelasticity determination method.
Keywords: Glass; Viscoelasticity; Creep testing; Relaxation modulus; TMA.

1. Introduction

Precision Glass Molding (PGM), as shown in Fig. 1, is a replicative process for mass-producing lenses of various shapes in a large volume for high end precision optical applications [1–3]. Glass molding process strongly depends on the mechanical and thermal properties of glass material, among which the viscoelasticity is most important for achieving a precise shape transfer from the mold [4,5]. Recently numerical method has become an efficient method to investigate glass molding process if accurate viscoelasticity data of glass is available [5,6]. Therefore, an accurate measurement method for viscoelastic properties of glass at certain temperature is critically needed.

For viscoelasticity measurement of glasses and other viscoelastic materials, the testing method can be mainly divided into two categories: dynamic method and static method [7,8]. In dynamic method, typically referred as dynamic thermo-mechanical analysis (DMA) [9], a sinusoidal stress is applied and the strain in the material is measured through DMA equipment, allowing one to determine the viscoelastic behavior of material. Static method can be further divided into two methods: creep test and stress relaxation test [10–13]. In creep test, after applying a

#376165 https://doi.org/10.1364/OE.28.000626
Journal © 2020 Received 29 Aug 2019; revised 2 Dec 2019; accepted 3 Dec 2019; published 3 Jan 2020

Optics EXPRESS

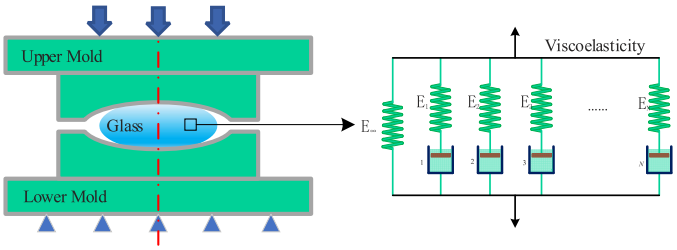

Fig. 1. Illustration of precision glass lens molding and viscoelasticity.

constant stress on glass at a certain temperature, the creep compliance will increase with time, and the modulus relaxation function can be converted from the creep compliance [14]. In stress relaxation test, an initial deformation is instantaneously applied to the sample and then kept at the last position, the decreasing stress as a function of time is measured to calculate the modulus relaxation function [15,16].

Although both dynamic and static methods can measure viscoelasticity of glass material, there are still some challenges in measuring viscoelasticity accurately, especially at high temperatures. For dynamic method, the general DMA equipment used to measure the viscoelastic properties is not suitable to evaluate the glass having a transition temperature over 500°, because the equipment is generally designed for plastic material, and its upper limit for the measurement temperature is mostly at 300–400° [17]. For stress relaxation testing method, it's difficult to impose an ideal instantaneous deformation to the specimen [16], and subsequently, the ideal testing condition of the stress relaxation can't be acquired. Therefore, compared with the methods mentioned above, creep testing method, especially cylinder compression creep testing [5,18], is more inclined to be used to measure viscoelastic properties [4,16,17]. However, when cylinder specimen compresses with a constant load, it will expand in the radial direction, and inconstant stress will be induced and an estimation error of the creep compliance function will occur. Besides, existed calculation method has limitation in transforming creep data to viscoelasticity data, especially when Poisson's ratio is unknown in molding temperature, which further induce a block to characterize viscoelastic parameter. Therefore, an ideal testing and easy implemented calculation method need to be developed to have high accuracy viscoelastic data of glass material, with more convenience.

2. Basic theory of viscoelasticity

In high precision glass molding process, glass flow in the mold under pressure is not purely elastic or viscous deformation, and its response to die pressure has the combination of viscosity and elasticity properties, called viscoelastic behavior [19–21]. The viscoelastic stress-strain equation not only depends on the current stress and strain state, but also depends on the entire development history of these states. This constitutive behavior could be expressed by hereditary or Duhamel integrals which are formed by taking the stress or strain accumulation with time into account [22].

For an isotropic viscoelastic material, the deviatoric and volumetric behaviors are considered fully decoupled [22], as shown in Fig. 2, and the constitutive relation of relaxation form are given

Optics EXPRESS

by [16,22]

$$\begin{aligned}\sigma_{ij}(t) &= e_{ij}(0)\cdot 2G(t) + \int_0^t e_{ij}(t')\frac{d2G(t-t')}{d(t-t')}dt' \\ &+\delta_{ij}\cdot e_{ii}(0)\cdot 3K(t) + \delta_{ij}\cdot\int_0^t e_{ii}(t')\frac{d3K(t-t')}{d(t-t')}dt' \\ &= S_{ij}(t) + \sigma_{ii}(t), (i,j=1,2,3)\end{aligned} \quad , \tag{1}$$

where δ_{ij} is the Kronecker symbol, S_{ij} and σ_{ii} are deviatoric and volumetric stresses, respectively, e_{ij} and ε_{ii} are deviatoric and volumetric strains, respectively, and $G(t)$, $K(t)$ are deviatoric and volumetric relaxation moduli which represent the response to a unit applied strain and have characteristic relaxation time. The relaxation moduli for materials with a fading memory can be expressed in terms of Prony or exponential series [19,22].

$$G(t) = G_\infty + \sum_{i=1}^{N_1} G_i exp(-t/\tau_i), \tag{2}$$

$$K(t) = K_\infty + \sum_{j=1}^{N_2} K_j exp(-t/\lambda_j), \tag{3}$$

In the equations above, G_∞ and K_∞ are the long term shear and bulk modulus, τ_i and λ_i are the corresponding relaxation time for the deviatoric and volumetric relaxation moduli. The short term moduli which describe the instantaneous elastic response given by [19,22,23]

$$G_0 = G_\infty + \sum_{n=1}^{N} G_n, \tag{4}$$

$$K_0 = K_\infty + \sum_{n=1}^{N} K_n, \tag{5}$$

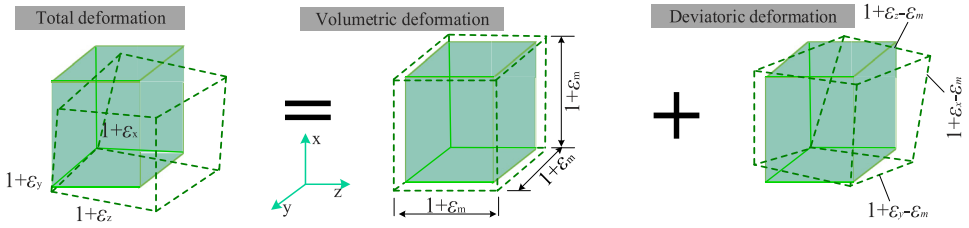

Fig. 2. Illustration of material deformation including deviatoric and volumetric behavior.

3. Minimal uniaxial creep testing (MUCT) method

In creep test, after applying a constant stress on glass at a certain temperature, the strain will increase with time. However, as seen in Fig. 3 of a traditional uniaxial creep testing, cross-sectional area becomes much larger due to uniaxial displacement, which will lead to declining compressive stress, and the cylinder shape becomes bulging due to contact surface friction [16,17]. In practice, the larger uniaxial displacement, the larger cross-section and the more bulging shape becomes.

Inspired by this observation, if we can keep minimal uniaxial shift, the cylinder section can be considered as unchanged, and then compressive stress can be guaranteed as constant.

Optics EXPRESS

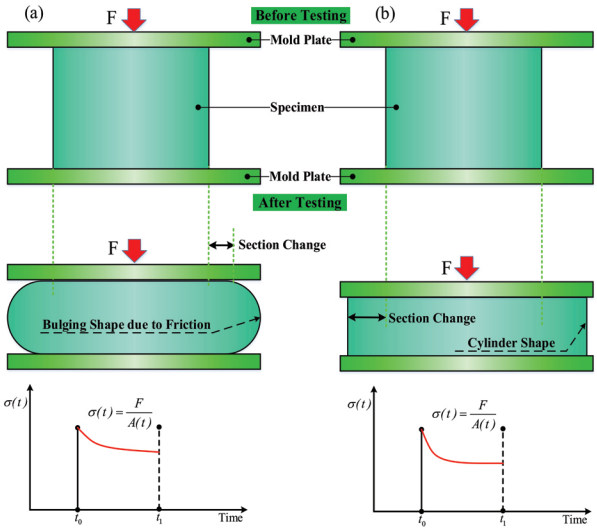

Fig. 3. Traditional uniaxial creep testing processes with friction in interface (a) and without friction in interface (b).

Furthermore, cylinder shape can be considered as non-bulging, so the friction effect should be weakened. This will meet our requirement to realize a more idealized creep testing. In order to keep minimal shift during uniaxial creep testing, a creep test scheme based on thermo-mechanical analysis (TMA) instrument is designed. For TMA equipment, it is based on the measurement of specimen length change under negligible load at scanned temperature [24,25], and every change of length in the sample is communicated to a highly sensitive inductive displacement transducer (LVDT) via a push rod and transformed into a digital signal. It is usually used to determine the physical or chemical properties of the specimen as it is heated, cooled or held at constant temperature [26]. For example, the thermal expansion and transition temperature properties of glass material can be measured [26–28]. With the improvement of sensor technology [29], the TMA instrument can achieve the resolution up to 0.5 nanometer. Besides, the force generator of TMA works electromagnetically, and, after an electric current is applied in the magnetic field, the force can be generated instantaneously. This means TMA can achieve more idealized step loading than traditional pressing equipment (produce force by motor), with very short ramp up time, further improving the measurement accuracy.

The detailed uniaxial creep testing scheme of this study is illustrated in Fig. 4, where the glass specimen is sandwiched between two-cylinder plate sapphire molds with 12.5mm in diameter and 0.55mm in thickness to prevent the adhesion between the glass and the quartz carrier of the test equipment. The borosilicate glass 3.3 specimen is machined to a cylinder shape with 2.5mm in height and 8mm in diameter. Both surfaces of glass specimen and sapphire plate are polished to further minimize the friction effects, qualities of polished surfaces are measured by Zygo white-light interferometer system, and roughness values of these surfaces are illustrated in Fig. 5. Table 1 summarizes material properties of borosilicate glass 3.3, quartz and sapphire.

Since the shift is controlled within several thousandths of total displacement in this creep test, usually just several microns, and nanometer resolution can be achieved, this method could be called minimal uniaxial creep testing (MUCT) method for measuring viscoelasticity properties.

Optics EXPRESS

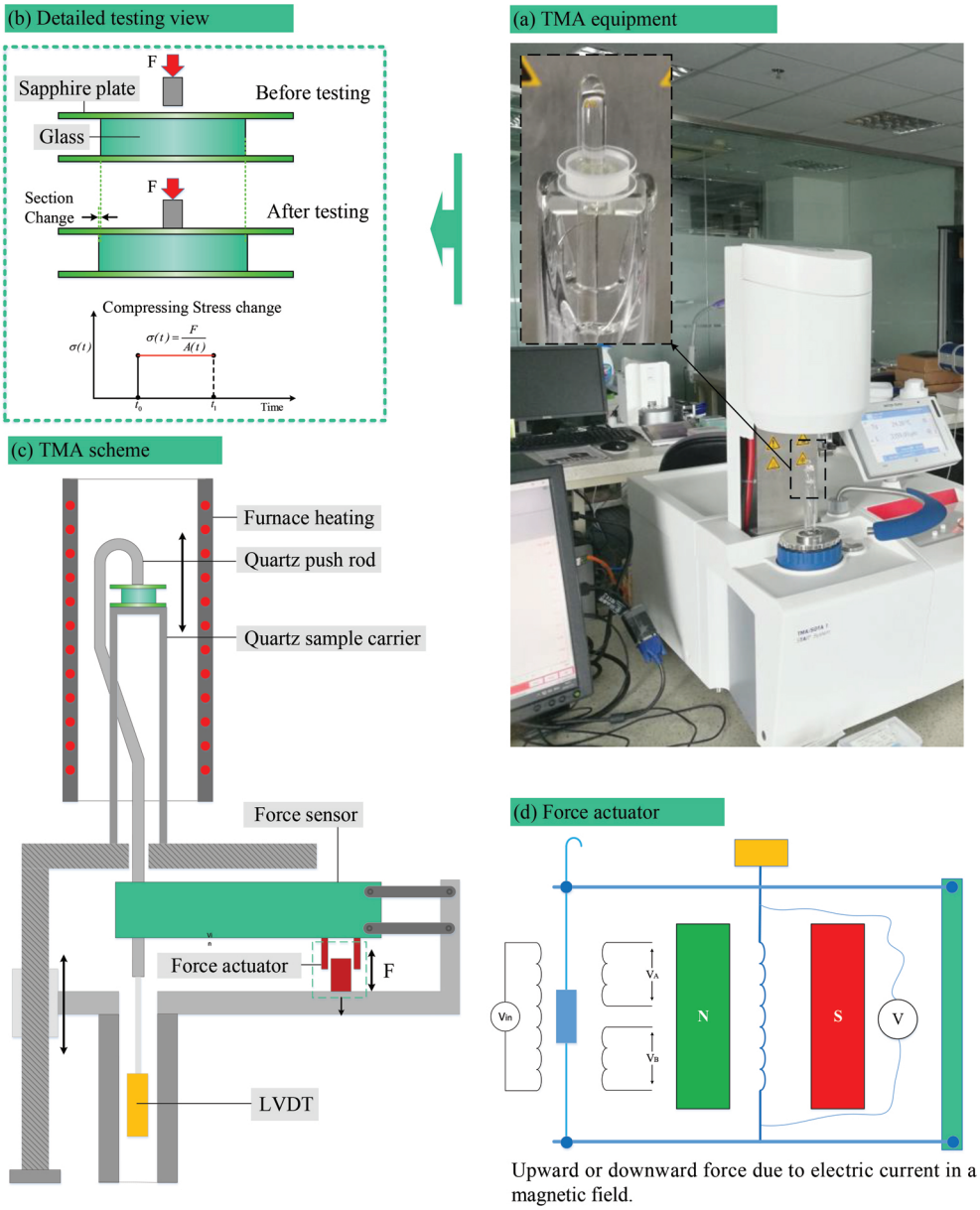

Fig. 4. The TMA equipment (a), detailed testing view (b), the TMA scheme (c), and force actuator (d).

Optics EXPRESS

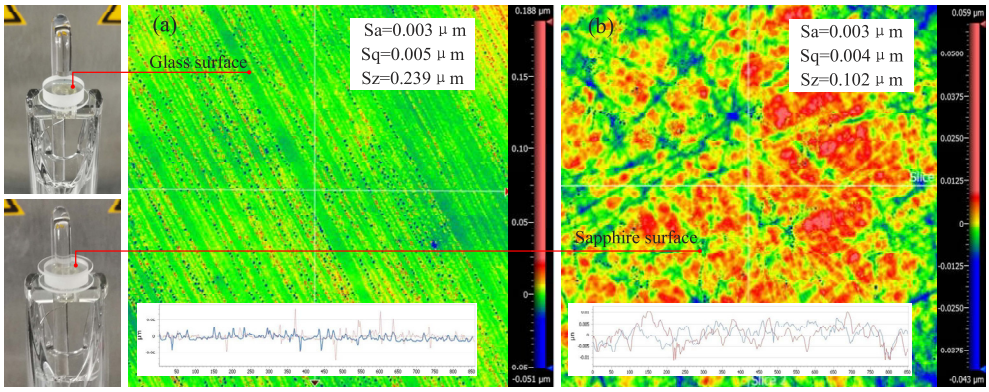

Fig. 5. Surface finish of glass specimen (a) and sapphire plate (b).

Table 1. Material properties of borosilicate glass 3.3, quartz and sapphire

Physical Characteristics	Borosilicate Glass	Quartz	Sapphire
Thermal expansion a (20°C; 300°C), K^{-1}	3.3×10^{-6}	5.5×10^{-7}	8.4×10^{-6}
Transformation temperature Tg °C	525	1200	—
Softening point °C	825	1730	—
Density at 25°C, g·cm^{-3}	2.2	2.7	3.98
Young's modulus E at 25°C, KN·mm^{-2}	64	76.5	350
Poisson's ratio μ at 25°C	0.2	0.17	0.29
Thermal conductivity w at 90°, C W·m^{-1}·K^{-1}	1.2	1.4	6.05

4. Determination of modulus relaxation function

4.1. Proposing a new calculation method on viscoelasticity determination

For linear viscoelastic material under uniaxial (x-direction) compressive stress condition, the constitutive equation for deviatoric stress component $S_{11}(t)$ in this direction can be expressed by [30]

$$\begin{aligned} S_{11}(t) &= 2G(t)\cdot e_{11}(0) + \int_0^t 2G(t-t')\cdot\frac{de_{11}(t')}{d(t')}dt' \\ &= 2G(t)\cdot[\varepsilon_x(0)-\varepsilon_m(0)] + \int_0^t 2G(t-t')\frac{d[\varepsilon_x(t')-\varepsilon_m(t')]}{d(t')}dt' \end{aligned}, \tag{6}$$

where $\varepsilon_x(t)$ is total strain in x-direction, $G(t)$ and $e_{11}(t)$ are shear relaxation modulus and principal deviatoric strain of x-direction respectively. Accordingly, volumetric stress $\sigma_m(t)$ can be expressed by

$$\sigma_m(t) = 3K(t)\cdot\varepsilon_m(0) + \int_0^t 3K(t-t')\frac{d\varepsilon_m(t')}{d(t')}dt', \tag{7}$$

where $K(t)$ and $\varepsilon_m(t)$ are bulk relaxation modulus and volumetric strain respectively.

The uniaxial response weakly depends on the volumetric relaxation [30], because the volumetric modulus only changes slightly and could be treated as a constant without relaxation behavior [16,17,30], while shear relaxation modulus could decrease to almost zero instantly [30,31]. Therefore, compared with total uniaxial strain $\varepsilon_x(t)$, volumetric strain $\varepsilon_m(t)$ could be neglected.

Optics EXPRESS

Equation (6) could be transformed to

$$S_{11}(t) = 2G(t) \cdot \varepsilon_x(0) + \int_0^t 2G(t-t')\frac{d\varepsilon_x(t')}{d(t')}dt'. \tag{8}$$

In uniaxial compression creep experiment, the stress component of uniaxial direction includes both deviatoric stress and dilatational stress as

$$\sigma_x(t) = S_{11}(t) + \sigma_m(t). \tag{9}$$

According to the first principal invariant of deviatoric stress tensor [32], dilatational stress $\sigma_m(t)$ is one third of the first invariant $I_1(t)$, and can be expressed by

$$\sigma_m(t) = \frac{1}{3}I_1(t) = \frac{1}{3}[\sigma_1(t) + \sigma_2(t) + \sigma_3(t)]. \tag{10}$$

In uniaxial compression creep experiment, $\sigma_y(t) = \sigma_z(t) = 0$, therefore

$$\sigma_m(t) = \frac{1}{3}\sigma_x(t). \tag{11}$$

According to Eqs. (9) and (11), there is

$$S_{11}(t) = \sigma_x(t) - \sigma_m(t) = \frac{2}{3}\sigma_x(t). \tag{12}$$

Combining Eqs. (8) and (12), there will be

$$S_{11}(t) = \frac{2}{3}\sigma_x(t) = 2G(t) \cdot \varepsilon_x(0) + \int_0^t 2G(t-t')\frac{d\varepsilon_x(t')}{d(t')}dt'. \tag{13}$$

According to the linear viscoelastic theory [30], uniaxial strain $\varepsilon_x(t)$ can be expressed by the following convolution integral equation:

$$\varepsilon_x(t) = J_x(t) \cdot \sigma_x(0) + \int_0^t J_x(t-t')\frac{d\sigma_x(t')}{d(t')}dt'. \tag{14}$$

Applying Laplace transform to Eqs. (13) and (14), then

$$\bar{S}_{11}(s) = \frac{2}{3}\bar{\sigma}_x(s) = 2s\bar{G}(s)\bar{\varepsilon}_x(s), \tag{15}$$

$$\bar{\varepsilon}_x(s) = s\bar{J}_x(s)\bar{\sigma}_x(s). \tag{16}$$

Then, the relationship between shear relaxation modulus function $\bar{G}(s)$ and uniaxial creep compliance function $\bar{J}_x(s)$ can be simplified as follows:

$$2\bar{G}(s) = \frac{2}{3} \cdot \frac{1}{s^2\bar{J}_x(s)}. \tag{17}$$

This indicates that shear relaxation modulus $\bar{G}(s)$ can be derived from uniaxial creep compliance $\bar{J}_x(s)$ directly, whereby $G(t)$ can be obtained by using inverse Laplace transform. Compared with $2\bar{G}(s) = 2 \cdot 3 \cdot \overline{K}(s)\overline{E}(s)[9\overline{K}(s) - \overline{E}(s)]^{-1}$ [16,17,33], a widely used shear relaxation determination equation, the proposing calculation method shown in Eq. (17) can be used to derive shear relaxation modulus without knowing information about bulk modulus and Poisson's ratio, which is due to shear relaxation dominating in uniaxial creep deformation [30]. Therefore, the proposing shear calculation method extends the application range, especially when Poisson's ratio and bulk modulus are unknown at a certain temperature.

Optics EXPRESS

4.2. Measurement of the creep function curve in MUCT process

In MUCT process, glass specimen is heated up to 650°C above Tg, and is soaked for a sufficiently long time in order to reach homogeneous temperature distribution. After heating, with temperature keeping at 650°C, an instantaneous step load of 0.5 N is applied to the specimen, and test duration is maintained for a sufficient period of time in order to have sufficient data points in displacement curve.

For a linear viscoelastic material, if it is subjected to a constant uniaxial stress σ_0 at time t_0, its strain $\varepsilon_x(t)$ rises instantaneously to the elastic value $\varepsilon_E = \sigma_0 / E_0$, then gradually to a maximum value of delayed elastic strain ε_D, and finally to an irreversible linear strain caused by viscous flow, as shown in Fig. 6(a) [30].

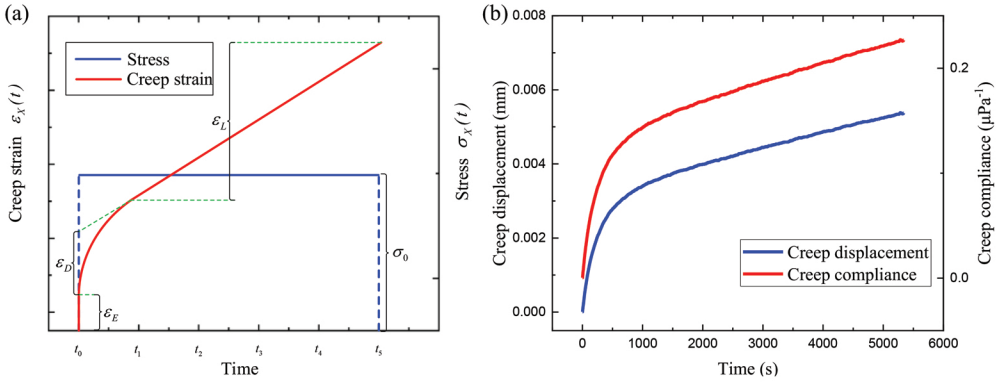

Fig. 6. Ideal uniaxial creep strain curve for viscoelastic material (a) and uniaxial creep strain curve and creep compliance curve obtained by MUCT method (b).

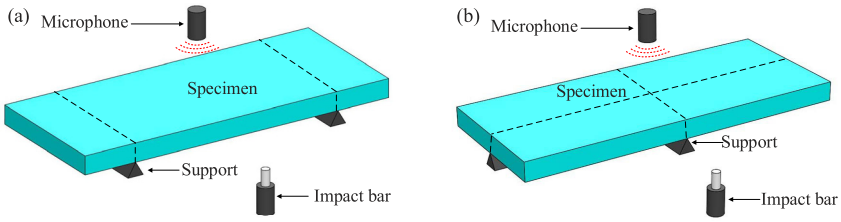

Fig. 7. IET testing for Young's modulus(a) and the shear modulus (b).

After testing, uniaxial creep strain curve and corresponding creep compliance curve are obtained and plotted in Fig. 6(b), where the creep compliance curve is directly calculated by $J_x(t) = \varepsilon_x(t) \cdot \sigma_x^{-1}$. It has been clearly shown that the uniaxial creep strain curve measured by MUCT in Fig. 6(b) has the same trend with the ideal one in Fig. 6(a).

4.3. Calculation of shear relaxation modulus function

Uniaxial creep compliance testing data could be fitted by a generalized Voigt model $J_x(t)$ in Prony series as the following equation:

$$J_x(t) = \frac{1}{E_0} + \sum_{i=1}^{n} \frac{1}{E_i}(1 - e^{-t/\tau_i^*}). \tag{18}$$

Optics EXPRESS

Where E is the Young's modulus that is temperature-dependent, and E_i and τ_i are the elastic modulus relaxation time of each Kelvin component, respectively. The uniaxial creep compliance curves of input (testing) and output (fitting) are shown in Fig. 8(a).

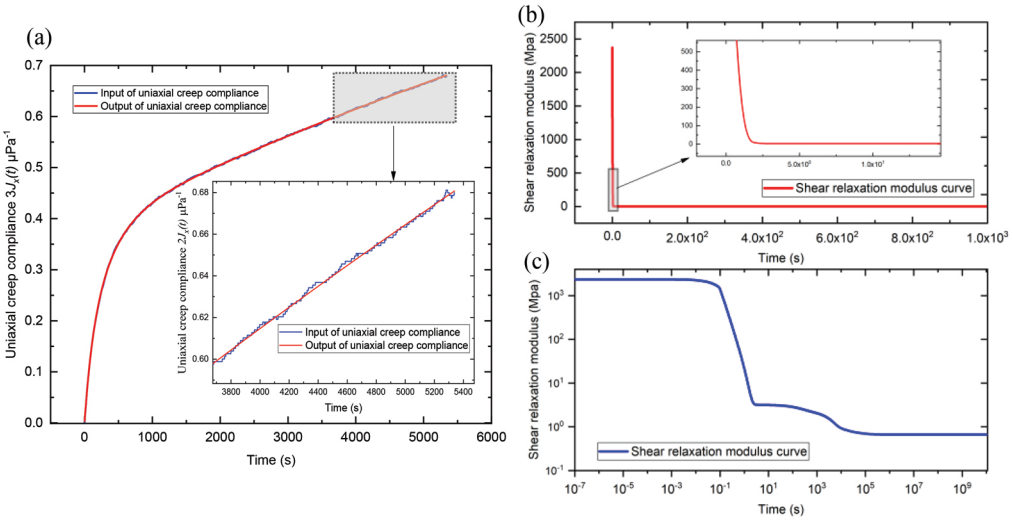

Fig. 8. Uniaxial creep compliance curve of input (testing) and output (fitting) (a), calculated shear stress relaxation modulus function curve in normal time scale (b) and in log time scale (c).

By applying Laplace transform to Eq. (18), we have the Laplace-transformed creep function $\bar{J}_x(s)$:

$$\bar{J}_x(s) = \frac{1}{sE_0} + \sum_{i=1}^{n} \frac{1}{sE_i(1 + s\tau_i^*)}. \tag{19}$$

As described previously, the shear relaxation modulus $\bar{G}(s)$ in the Laplace transformed domain can be calculated by Eq. (17). Substituting Eq. (19) into Eq. (17), the Laplace transformed shear relaxation modulus can be derived as:

$$2\bar{G}(s) = \frac{2}{3} \cdot \frac{1}{s^2\bar{J}_x(s)} = \frac{2}{3} \cdot \frac{1}{\left[\frac{s}{E_0} + \sum_{i=1}^{n} \frac{s}{E_i(1 + s\tau_i^*)}\right]}. \tag{20}$$

A generalized Maxwell model with six Prony series is employed to express shear relaxation modulus $G(t)$, since model with six Prony series (or more than six) can sufficiently describe the relaxation modulus spectrum of glass viscoelasticity at certain temperature [30,34]. In this model, the shear relaxation modulus $G(t)$ [23] is expressed below:

$$G(t) = G_\infty + \sum_{i=1}^{6} G_i exp(-t/\tau_i), \tag{21}$$

where $\tau_i = \eta_i / G_i$ is shear stress relaxation time, G_i and G_∞ denote, respectively, shear modulus component and long-term shear modulus. By using the relationship mentioned in Eq. (20) and the inverse Laplace transform, shear relaxation modulus $G(t)$ with six Prony series is specified, and the specific coefficients are listed in Table 2.

In real uniaxial creep deformation testing, the elastic strain $\varepsilon_E = \sigma_0 / E$ as shown in Fig. 6(a) includes not only elastic strain of specimen but also elastic strain from support and pressing

Optics EXPRESS

Table 2. Coefficient of shear relaxation modulus in 650°

Shear modulus G_i *(MPa)*			Prony factor g_i		
G_1	G_2	G_3	g_1	g_2	g_3
788.299	789.291	789.788	3.325×10^{-1}	3.330×10^{-1}	3.332×10^{-1}
G_4	G_5	G_6	g_4	g_5	g_6
0.011	0.811	1.709	4.638×10^{-6}	3.420×10^{-4}	7.208×10^{-4}
Stress relaxation times τi *(s)*			Short term and Long-term shear modulus *(MPa)*		
τ_1	τ_2	τ_3	Short term shear modulus G_0		
2.110×10^{-1}	2.121×10^{-1}	2.292×10^{-1}	2370.580		
τ_4	τ_5	τ_6	Long term shear modulus G_∞		
1.687×10^{2}	2.087×10^{2}	4.628×10^{3}	0.667		

mold, which makes all elastic strains mixed up together, and this unreal elastic strain is neglected by TMA data processing software at test beginning. On this account, the calculated short-term modulus by uniaxial creep testing method is not equal to the real short-term modulus. Finally, as shown in Table 2, the calculated short-term shear modulus at 650 °C is 2.37 GPa.

In order to know the real value of short modulus of borosilicate glass 3.3 at 650 °C, impulse excitation technique (IET) can be used to implement the direct measurement. Figure 7 shows two typical testing modes (flexural mode and torsional mode) and how to support the specimen in each mode to minimize the frictional effects at supports. During testing, the sample (70 mm × 25 mm × 6 mm) is tapped by an impact bar, and a sensor records the induced vibration signals. The acquired vibration signal in the time domain is then converted to the frequency domain by a fast Fourier transformation. One can then determine the resonant frequency with high accuracy to calculate the elastic properties based on classical beam theory. Finally, the short-term shear modulus value tested by IET is 25.7 GPa, which is different from the calculated value of 2.37 GPa. Given this difference, the influence of short-term modulus' on glass rheology can be performed by analyzing the shear relaxation modulus function properties. More detail about IET equipment and testing process can be seen in Appendix A.

The calculated shear relaxation modulus function curves varying with time are plotted in Figs. 8(b) and 8(c). It can be observed that the shear modulus decays within seconds to a small value close to 1 MPa, in other words, at this temperature, the glass deformation should be almost independent on the short-term shear modulus and dominantly rely on the shear modulus with small value (after relaxation). Therefore, according to the shear relaxation modulus properties, it doesn't matter whether the short-term shear modulus is 2.37 GPa or 25.7 GPa for predicting the rheological behavior of glass on a larger time-scale at this temperature.

5. Validation of shear relaxation modulus function

5.1. Finite element model building for glass cylinder compression

A simulation model is built in FEM software MSC. Marc to verify the calculated shear relaxation modulus function by comparing measured and simulated creep testing data. Since the glass specimen and sapphire plate are in cylindrical shape, and both the thermal and mechanical loading conditions are axisymmetric, a simplified axisymmetric model is adopted, as illustrated in Fig. 9. An actual creep experiment involves the four stages: heating, soaking, pressing, and cooling. However, the testing data are only obtained at the pressing stage of a certain temperature, therefore other stages do not affect the results.

In the simulation model, the bottom sapphire plate is fixed, the constant load force and thermal conditions, which are same as actual situation, are applied. Shear relaxation modulus data and other material parameters are added to finite elements.

Optics EXPRESS

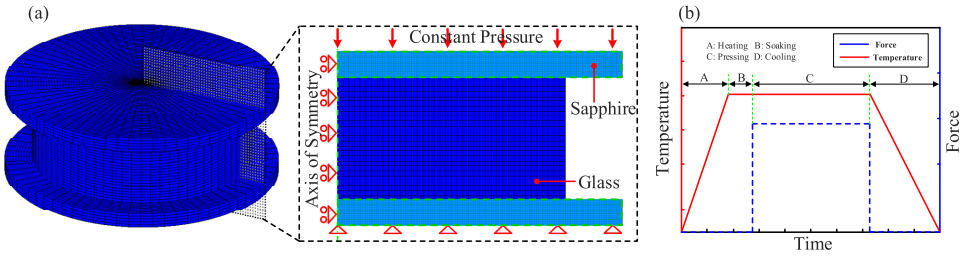

Fig. 9. Axisymmetric FEM model (a) and thermo-mechanical loading process (b).

5.2. *Validation of the determined viscoelasticity*

In ideal situation, if axial creep displacement can be achieved from test without compression stress change and interface friction, the calculated relaxation modulus will be much accurate. In the MUCT process, the section of the sample could be considered a constant, which means a constant compression stress could be guaranteed, and thus the interface friction will be the only remaining factor affecting the creep displacement result. In our previous study of frictional dependence and predictive accuracy of viscoelastic model [31], when the interface friction can't be slashed in real testing, the uniaxial creep displacement curve of simulation, reproduced by the frictional disturbed viscoelasticity, has a large deviation with the testing curve.

Since glass and sapphire surfaces are polished, the interface friction force should be very small or zero. Thus, in simulation, the interface friction coefficient is chosen as 0. If the simulated and experimental results are consistent, the determined viscoelasticity should be accurate. If not, friction might exist in the contact interface between mold and specimen in the deformation process, and friction compensation should be further studied.

With zero as the input of the interface friction coefficient, the simulated displacement cloud diagrams at the end of time are illustrated in Fig. 10. It is found that the axial displacements of all the points on one certain horizontal layer (i.e., Layer a) have the same value. Correspondingly, the rational displacements of all the points on one certain vertical layer (i.e., Layer b) are identical. Figure 11(a) shows the real-time creep displacements of the layers of a, b, c, and d. Overall, all the creep displacements of these layers are consistent in trend. The outer layer (i.e., Layer a and d) is two times higher than the corresponding middle one (i.e., Layer b and c) in creep displacement over the whole process. These means, without interface friction, each layer has a uniform deformation and the deformation is linearly proportional to the layer location. And in such situation (without friction), the uniaxial creep deformation should be ideal.

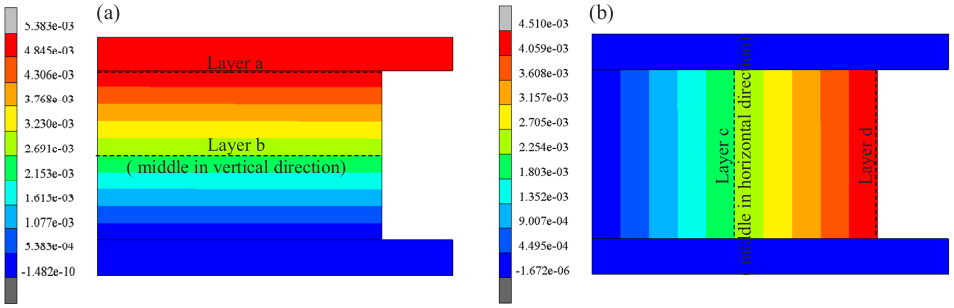

Fig. 10. Uniaxial displacement diagram (a), radial displacement diagram (b) of simulation.

Optics EXPRESS

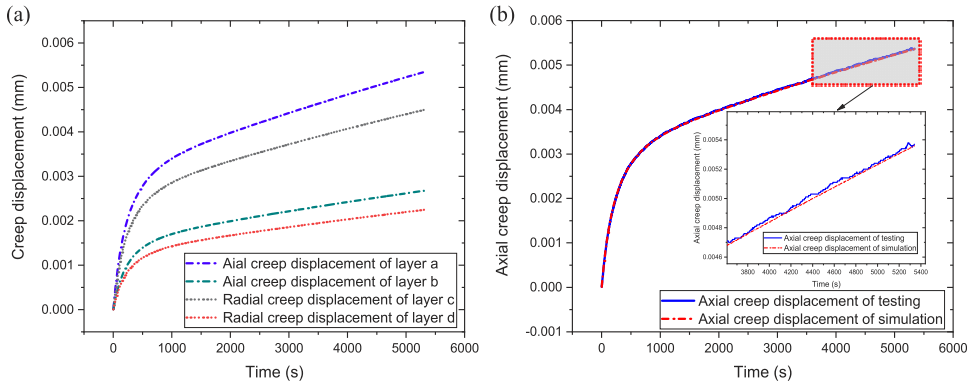

Fig. 11. Uniaxial displacement curve (a), radial displacement curve (b) of simulation.

To compare the accuracies of the simulation result with the testing one, the uniaxial creep displacement (layer a) of the simulation is plotted in Fig. 11(b), with the experimental result as comparison. As shown in Fig. 11(b), it is found that the uniaxial displacement curve of simulation is in great agreement with testing curve, with minor deviations. More specifically, the displacement curve of the simulation is just slightly lower than testing one in the whole process. The reason of the subtle deviations could be that the uniaxial deformation contributed by bulk modulus relaxation is neglected [18,31], in the viscoelasticity calculation process of section 4. That is, the minor deviations signify that the rheological deformation of the uniaxial creep testing should be dominantly contributed by shear modulus relaxation. Considering the high performance of consistency, MUCT method could be used as an ideal uniaxial creep testing method for glass viscoelasticity determination.

6. Conclusion

This study proposes a new testing and calculation method for determination glass viscoelasticity, and the conclusions of this study can be drawn as follows:

Firstly, a minimal uniaxial creep testing (MUCT) method based on TMA is proposed. Different from the traditional creep testing method, only a few microns of creep displacement occur during the process of MUCT, so the cross-section can be considered as unchanged, and the compressive stress can be considered as constant, which guarantees an ideal creep testing curve. Secondly, by analyzing shear relaxation modulus and bulk relaxation modulus behavior on the deformation process, a direct conversion method from uniaxial creep compliance to shear relaxation modulus is proposed. Compared with existed (traditional) shear relaxation determination equation, the proposing calculation method can be used to derive shear relaxation modulus without knowing information about bulk modulus and Poisson's ratio. Accordingly, this method extends the application range, especially when Poisson's ratio or bulk modulus are unknown at a certain temperature. Thirdly, according to the function curve property of the calculated shear relaxation modulus, it can be observed that the shear modulus drops significantly within seconds to a minor amount (close to 1 MPa). In other words, at this temperature, the glass deformation should be almost independent on short-term shear modulus and dominantly relied on the relaxed shear modulus after a sharp decrease. In the end, the accuracy of the determined viscoelasticity is verified by finite element simulation. According to the analysis result, the simulation curve and experimental curve coincide greatly, thus MUCT method could be used as a high accuracy viscoelasticity testing approach.

Optics EXPRESS

Appendix A

A.1 The process of measurement of instantaneous elastic properties by IET in high temperature

The borosilicate glass specimen is suspended in platinum-rhodium (PtRh)-wires that are fixed to parallel Al_2O_3 support units, since PtRh and Al_2O_3 have good high-temperature and oxidation resistance. The support unit with the glass specimen is then moved in the furnace, while the non-contact transducer is placed above an anti-node point of the test specimen to pick up the desired vibration, but not so close as to affect the free vibration.

Then the specimen is stroked lightly and elastically by an impact bar, either at the center of the specimen for flexural mode or at the quadrant for torsion mode correspondingly, as shown in Fig. 12(a). Meanwhile, the sample's temperature is raised from 25 °C to 650 °C at a heating rate of 2 °C/min. The vibration signal is constantly recorded by the microphone and transformed to the signal system for analysis.

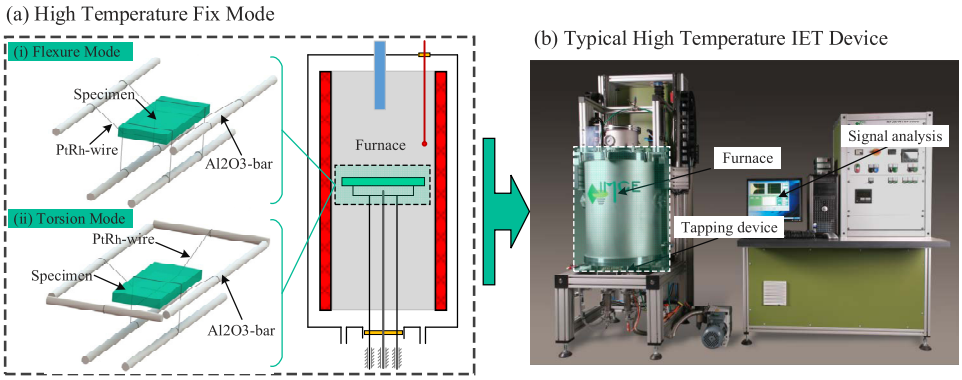

Fig. 12. Fix mode (a) and typical high temperature IET device (b).

Young's modulus value can be determined using the resonant frequency in the flexural mode of vibration. For a rectangular specimen in flexure mode, the dynamic Young's modulus can be calculated from Eq. (23) [35]:

$$E = 0.9465\left(\frac{mf_f^2}{W}\right)\left(\frac{L^3}{H^3}\right)\delta. \tag{23}$$

where m, W, L and H are the mass, width, length, and thickness of the specimen respectively, and f_f is the fundamental frequency of vibration in flexure mode. δ factor for the fundamental flexural mode to account for the length-to-thickness ratio of the specimen, Poisson's ratio, and so forth. In the present work, the value δ is calculated by an expression used for the rectangular geometry bar [35,36],

$$\delta = 1 + 6.585[1 + 0.0752\mu + 0.8109\mu^2]\left(\frac{H}{L}\right)^2 - 0.868\left(\frac{H}{L}\right)^4 - \frac{8.340(1+0.2023\mu+2.173\mu^2)(H/L)^4}{1+6.338(1+0.1408\mu+1.536\mu^2)(H/L)^2}. \tag{24}$$

where μ is Poisson's ratio.

Optics EXPRESS

Shear modulus can be determined by the torsional resonant frequency, the mass and dimensions of a rectangular bar according to the ASTM standards in Eq. (25) [35]:

$$G = \frac{4Lmf_t^2}{WH}R, \tag{25}$$

where f_t, m, L and H are the fundamental torsional resonant frequency, mass, width, length and thickness of the specimen, respectively. R is the correction factor for fundamental torsional mode, its value can be calculated by Eq. (26) [35]

$$R = \left[\left(1 + (W/H)^2\right) \Big/ \left(4 - 2.521\frac{H}{W}\left(1 - 1.991 \Big/ e^{\pi\frac{W}{H}} + 1\right)\right)\right]\left[1 + \frac{0.00851n^2W^2}{L^2}\right] - 0.060\left(\frac{W}{L}\right)^{\frac{3}{2}}\left(\frac{W}{H} - 1\right)^2, \tag{26}$$

When calculating Young's modulus and shear modulus, Poisson's ratio μ in relevant solution equations is usually not known at first, so these equations cannot be used directly. Especially, according to ASTM Standards [35], if $L/H < 20$ and Poisson's ratio is unknown, an initial Poisson's ratio μ0 can be assumed to begin the calculation. Then through an iterative process as shown in Fig. 13, the final estimated Poisson's ratio, Young's modulus, and shear modulus can be obtained. In addition, the bulk modulus can be obtained by $K = GE/(3(3G - E))$.

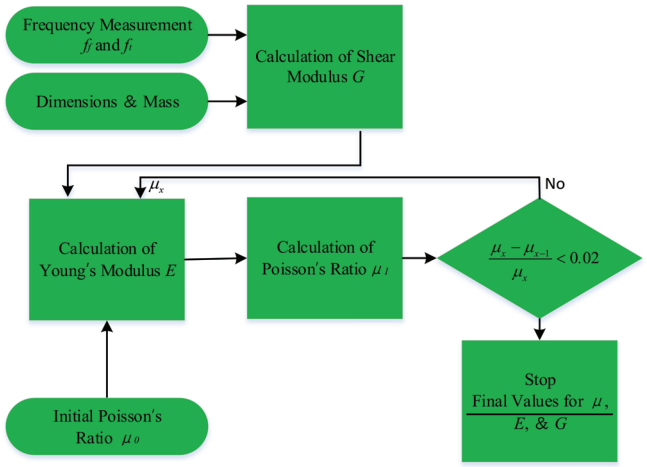

Fig. 13. Process Flow Chart for Iterative Determination of Elastic Properties

Funding

International Science and Technology Cooperation Programme (2017YFE0116900); Hunan Advanced Composite Manufacturing International Science and Technology Innovation Cooperation Base; China Scholarship Council(201806130148).

Acknowledgments

Yingying Zhang acknowledges the experiment support from Mettler-Toledo Company.

References and links

1. G. Yan, Y. Zhang, K. You, Z. Li, Y. Yuan, and F. Fang, "Off-spindle-axis spiral grinding of aspheric microlens array mold inserts," Opt. Express **27**(8), 10873–10889 (2019)..

Optics EXPRESS

2. Y. Zhang, G. Yan, Z. Li, and F. Fang, "Quality improvement of collimating lens produced by precision glass molding according to performance evaluation," Opt. Express **27**(4), 5033–5047 (2019)..
3. Y. K. Kim, J. H. Ju, and S.-M. Kim, "Replication of a glass microlens array using a vitreous carbon mold," Opt. Express **26**(12), 14936–14944 (2018)..
4. N. Kitamura, "Compression creep and dynamic viscoelastic studies of binary sodium and lithium silicate glasses around deformation temperature," J. Ceram. Soc. Jpn. **125**(10), 721–727 (2017)..
5. D. Joshi, P. Mosaddegh, J. D. Musgraves, K. C. Richardson, and P. F. Joseph, "Thermo-mechanical characterization of glass at high temperature using the cylinder compression test. Part I: Viscoelasticity, friction, and PPV," J. Rheol. **57**(5), 1367–1389 (2013)..
6. T. D. Pallicity, A. T. Vu, K. Ramesh, P. Mahajan, G. Liu, and O. Dambon, "Birefringence measurement for validation of simulation of precision glass molding process," J. Am. Ceram. Soc. **100**(10), 4680–4698 (2017)..
7. R. S. Lakes, "Viscoelastic measurement techniques," Rev. Sci. Instrum. **75**(4), 797–810 (2004)..
8. R. Murugan, R. Ramesh, and K. Padmanabhan, "Investigation on Static and Dynamic Mechanical Properties of Epoxy Based Woven Fabric Glass/Carbon Hybrid Composite Laminates," Procedia Eng. **97**, 459–468 (2014)..
9. R. P. Chartoff, J. D. Menczel, and S. H. Dillman, "Dynamic mechanical analysis (DMA)," Thermal analysis of polymers: fundamentals and applications. Wiley, San Jose 387–496 (2009).
10. D. D. Magura, M. A. Sozen, and C. P. Siess, "A study of stress relaxation in prestressing reinforcement," (University of Illinois Engineering Experiment Station. College of Engineering. University of Illinois at Urbana-Champaign., 1962).
11. H. Gjestland, G. Nussbaum, G. Regazzoni, O. Lohne, and Ø. Bauger, "Stress-relaxation and creep behaviour of some rapidly solidified magnesium alloys," Mater. Sci. Eng., A **134**, 1197–1200 (1991)..
12. R. M. Guedes, A. T. Marques, and A. Cardon, "Analytical and experimental evaluation of nonlinear viscoelastic-viscoplastic composite laminates under creep, creep-recovery, relaxation and ramp loading," Mech. Time-Depend. Mater. **2**(2), 113–128 (1998)..
13. G. Thornton, C. Frank, and N. Shrive, "Ligament creep behavior can be predicted from stress relaxation by incorporating fiber recruitment," J. Rheol. **45**(2), 493–507 (2001)..
14. T. Zhou, J. Yan, J. Masuda, and T. Kuriyagawa, "Investigation on the viscoelasticity of optical glass in ultraprecision lens molding process," J. Mater. Process. Technol. **209**(9), 4484–4489 (2009)..
15. A. Jain and A. Y. Yi, "Numerical Modeling of Viscoelastic Stress Relaxation During Glass Lens Forming Process," J. Am. Ceram. Soc. **88**(3), 530–535 (2005)..
16. J. Zhou, J. Yu, L. J. Lee, L. Shen, and A. Yi, "Stress Relaxation and Refractive Index Change of As2S3 in Compression Molding," Int. J. Appl. Glass Sci. **8**(3), 255–265 (2017)..
17. T. Kodera, "Characterization of the Thermo-Viscoelastic Property of Glass and Numerical Simulation of the Press Molding of Glass Lens," Journal of Thermal Stresses **32**(12), 1235–1255 (2009)..
18. D. Joshi, P. Mosaddegh, J. David Musgraves, K. C. Richardson, and P. F. Joseph, "Thermo-mechanical characterization of glass at high temperature using the cylinder compression test. Part II: No-slip experiments, viscoelastic constants, and sensitivity," J. Rheol. **57**(5), 1391–1410 (2013)..
19. ANSYS®Mechanical APDL theory reference (version 16.0).
20. A. C. Pipkin, *Lectures on viscoelasticity theory* (Springer Science & Business Media, 2012), Vol. 7.
21. A. D. Drozdov, *Finite elasticity and viscoelasticity: a course in the nonlinear mechanics of solids* (World Scientific, 1996).
22. Marc® Software Manual Volume A: Theory and User Information(Version 2018).
23. ABAQUS® Analysis User's Manual (Version 6.7).
24. K. Nakamura, E. Kinoshita, T. Hatakeyama, and H. Hatakeyama, "TMA measurement of swelling behavior of polysaccharide hydrogels," Thermochim. Acta **352-353**(352), 171–176 (2000)..
25. T. Hatakeyama and F. X. Quinn, *Thermal analysis : fundamentals and applications to polymer science* (John Wiley & Sons, 1999), pp. 485–487.
26. M. Wagner, *Thermal Analysis in Practice* (Mettler-Toledo, 2018).
27. S. W. Choi, H. S. Cho, and S. Kumai, "Influence of precipitation on the coefficient of thermal expansion of Al–Si–Mg–Cu–(Ti) alloys," J. Alloys Compd. **655**, 6–10 (2016)..
28. K. Backfolk, R. Holmes, P. Ihalainen, P. Sirviö, N. Triantafillopoulos, and J. Peltonen, "Determination of the glass transition temperature of latex films: Comparison of various methods," Polym. Test. **26**(8), 1031–1040 (2007)..
29. M. Wagner, "2 – A Brief History of Thermal Analysis," *Thermal Analysis in Practice* 16–18 (2018).
30. G. W. Scherer, *Relaxation in glass and composites* (Wiley, 1986).
31. J. Yu, H. Luo, Y. Zhang, T. V. Nguyen, X. Jiang, and J. Hu, "A comprehensive study on frictional dependence and predictive accuracy of viscoelastic model for optical glass using compression creep test," *Journal of the American Ceramic Society.*
32. F. Irgens, *Continuum mechanics* (Springer Science & Business Media, 2008).
33. M. L. Williams, R. F. Landel, and J. D. Ferry, "The temperature dependence of relaxation mechanisms in amorphous polymers and other glass-forming liquids," J. Am. Chem. Soc. **77**(14), 3701–3707 (1955)..
34. A. Sarhadi, J. H. Hattel, and H. N. Hansen, "Evaluation of the viscoelastic behaviour and glass/mould interface friction coefficient in the wafer based precision glass moulding," J. Mater. Process. Technol. **214**(7), 1427–1435 (2014)..
35. "ASTM E1876-15, Standard Test Method for Dynamic Young's Modulus, Shear Modulus, and Poisson's Ratio by Impulse Excitation of Vibration, ASTM International, West Conshohocken, PA, 2015, www.astm.org."

Optics EXPRESS

36. S. Spinner, "A method for determining mechanical resonance frequencies and for calculation elastic moduli from these frequencies," *Proc. ASTM* 1961, 1221–1238.